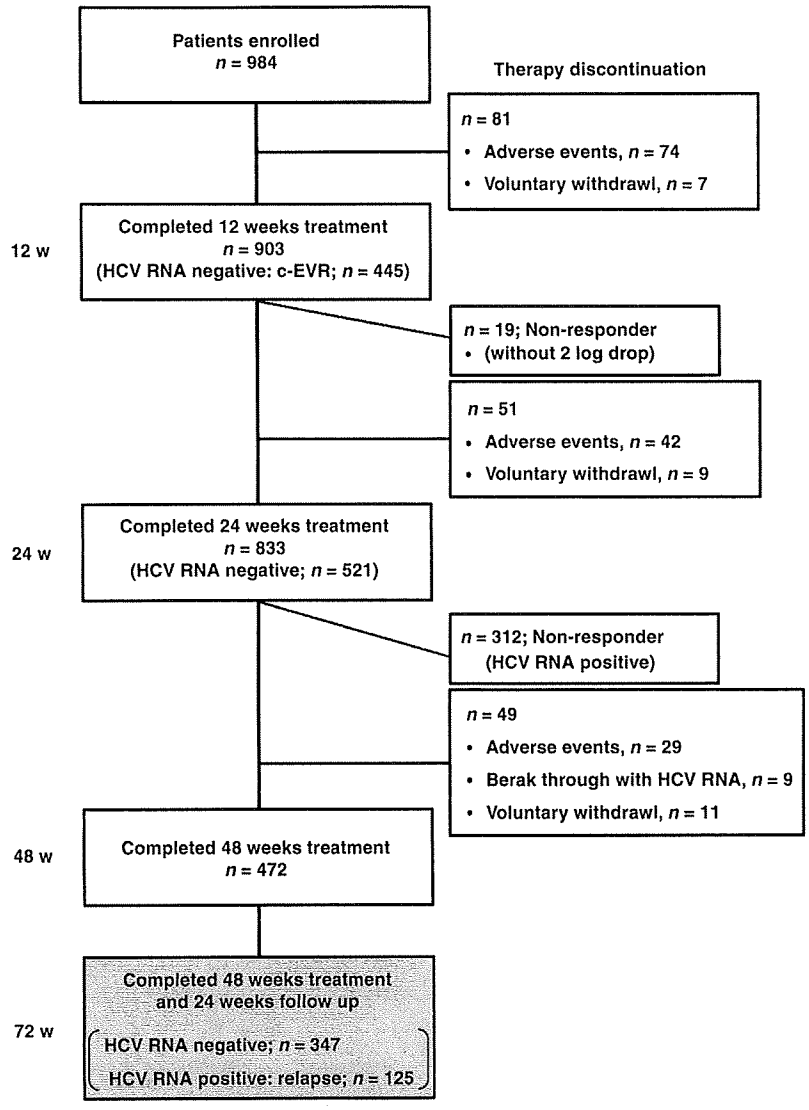

Fig. 1 Flow of patients throughout the study.

relapse rate was 60% (9/15) in patients receiving less than 6 mg/kg/day of ribavirin, and declined to 41% (32/79) at 6–8 mg/kg/day, 27% (34/124) at 8–10 mg/kg/day, 22% (43/193) at 10–12 mg/kg/day and 11% (7/61) in patients given ≥12 mg/kg/day ($P < 0.0001$). Figure 2 shows the relationship of the relapse rate and the mean ribavirin dose for two dosage groups of Peg-IFN α-2b: the group given ≥1.4 μg/kg/week of Peg-IFN and that given <1.4 μg/kg/week (1.4 μg/kg/week was the median value). In both groups, ribavirin was dose-dependently correlated with relapse. More than 12 mg/kg/day of the mean ribavirin exposure could suppress the relapse rate to 20% (4/20) in the group given <1.4 μg/kg/week and strongly suppress it to 7% (3/41) in the group given ≥1.4 μg/kg/week of Peg-IFN.

Impact of drug exposure during 0–48 weeks on relapse according to the timing of HCV RNA negativiation

Relapse rates among patients with c-EVR

The overall relapse rate among patients with c-EVR was 19% (75/391). We separately analysed the relapse rate among the patients with c-EVR according to the degree of exposure to both drugs. Table 3a shows the relapse rates among the patients with c-EVR according to the categories of Peg-IFN α-2b and ribavirin doses during the full treatment period. The relapse rate showed a decline according to the increase in the dose of ribavirin ($P = 0.0002$). The relapse rate was suppressed at an average of 15% (13–16%) in the patients who received 10–12 mg/kg/day of ribavirin, and the average was only 4% for those who received more than 12 mg/kg/day

Table 2 Factors associated with relapse among the patients with virologic response

(a) Univariate analysis

Factor	Nonrelapser	Relapser	*P* value
n	347	125	
Age (years)	53.9 ± 10.7	56.2 ± 9.2	0.07
Sex (male/female)	213/134	66/59	0.09
Serum HCV RNA (kIU/mL)*	1600	1800	0.34
White blood cells (/mm^3)	5335 ± 1517	5075 ± 1428	0.08
Neutrophils (/mm^3)	2797 ± 1143	2625 ± 1021	0.17
Red blood cells (×10^4/mm^3)	450 ± 45	446 ± 50	0.25
Haemoglobin (g/dL)	14.3 ± 1.4	14.2 ± 1.5	0.45
Platelets (×10^4/mm^3)	17.6 ± 5.3	16.4 ± 5.1	0.03
AST (IU/L)	60 ± 42	58 ± 33	0.75
ALT (IU/L)	75 ± 60	71 ± 50	0.98
Histology (METAVIR)†			
Fibrosis: 0–2/3–4	222/20	74/19	0.002
Activity: 0–1/2–3	140/102	52/41	0.75
Peg-IFN dose (μg/kg/week)‡	1.33 ± 0.26	1.27 ± 0.29	0.07
Ribavirin dose (mg/kg/day)‡	10.1 ± 1.9	9.1 ± 2.1	<0.001
Virologic response§: c-EVR/LVR	316/31	75/50	<0.001

(b) Multivariate analysis

Factor	Category	Odds ratio	95% CI	*P* value
Platelets	By 1 × 10^4/mm^3	–	–	NS
Fibrosis¶	0–2/3–4	1/3.192	1.515–6.725	0.002
Ribavirin dose‡	By 1 mg/kg/day	0.790	0.696–0.896	<0.001
Virologic response§	c-EVR/LVR	1/6.290	3.385–11.690	< 0.001

AST, aspartate aminotransferase; ALT, alanine aminotransferase; HCV, hepatitis C virus; c-EVR, complete early virologic response; LVR, late virologic response; NS, not significant difference Peg-IFN, pegylated interferon.
*Data shown are median values. †137 missing. ‡Mean doses during 0–48 weeks. §The timing of HCV RNA negativiation. ¶METAVIR fibrosis score.

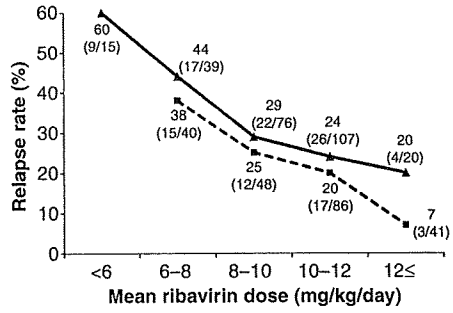

Fig. 2 Relapse rate according to Peg-IFN α-2b and ribavirin doses during treatment of patients who completed treatment, which was stratified with the mean ribavirin doses. (-▲-) Group with the mean Peg-IFN dose <1.4 μg/kg/week; (··■··) Group with the mean Peg-IFN dose ≥1.4 μg/kg/week. The ribavirin dose was dose-dependently correlated with the virologic relapse in both groups ($P < 0.0001$). There was no significant difference between the two Peg-IFN α-2b-dose groups ($P = 0.17$).

of ribavirin. In contrast, the relapse rate was not affected by the dose of Peg-IFN α-2b when the patients were given more than 0.9 μg/kg/week of Peg-IFN α-2b. On the other hand, with respect to patients with rapid virologic response (RVR) defined as the absence of detectable serum HCV RNA at treatment week 4 ($n = 41$), none showed relapse and all attained SVR irrespective of the dose of Peg-IFN α-2b or ribavirin (prevalence of patients: the mean dose of Peg-IFN α-2b; <0.9 : 0.9–1.2 : 1.2–1.5 : 1.5 μg/kg/week ≤ =7 : 17 : 34 : 42%, the mean dose of ribavirin; <8 : 8–10 : 10–12 : 12 mg/kg/day ≤ =15 : 24 : 41 : 20%).

Relapse rates among patients with LVR

Among the patients with LVR, the ribavirin exposure during treatment was also the factor correlated adversely with the relapse rate ($P = 0.03$). However, the overall relapse rate was 62% (50/81), which was much higher than that of the c-EVR patients ($P < 0.0001$) and 45% (5/11) of patients with LVR relapsed even in the group given more than 12 mg/kg/day of the average ribavirin dose (Table 3b).

Table 3 Relapse rate according to Peg-IFN and ribavirin doses during week 0–48 for patients with c-EVR and LVR who completed 48 weeks of treatment

(a) C-EVR

Peg-IFN dose (μg/kg/week)†	Ribavirin dose (mg/kg/day)*									
	12≤		10–12		8–10		<8		Total	
≥1.5	0%	(0/28)	13%	(4/31)	14%	(3/21)	29%	(5/17)	12%	(12/97)
1.2–1.5	20%	(2/10)	16%	(16/100)	25%	(16/65)	23%	(7/30)	20%	(41/205)
0.9–1.2	0%	(0/7)	13%	(2/15)	15%	(2/13)	38%	(6/16)	20%	(10/51)
<0.9	0%	(0/5)	15%	(2/13)	55%	(6/11)	44%	(4/9)	32%	(12/38)
Total	4%	(2/50)	15%	(24/159)	25%	(27/110)	31%	(22/72)	19%	(75/391)

(b) LVR

Peg-IFN dose (μg/kg/week)§	Ribavirin dose (mg/kg/day)‡									
	12≤		10–12		8–10		<8		Total	
≥1.5	43%	(3/7)	50%	(1/2)	100%	(2/2)	100%	(4/4)	67%	(10/15)
1.2–1.5		(1/1)	60%	(12/20)	29%	(2/7)	82%	(9/11)	62%	(24/39)
<1.2	33%	(1/3)	50%	(6/12)	60%	(3/5)	86%	(6/7)	59%	(16/27)
Total	45%	(5/11)	56%	(19/34)	50%	(7/14)	86%	(19/22)	62%	(50/81)

Peg-IFN, pegylated interferon; c-EVR, complete early virologic response; LVR, late virologic response.
*P = 0.0002 for comparison of the four ribavirin groups. †P = 0.08 for comparison of the four Peg-IFN groups. ‡P = 0.03 for comparison of the four ribavirin groups. §P = 0.57 for comparison of the three Peg-IFN groups.

Impact of dose reduction after week 12 on relapse among patients with c-EVR

Among c-EVR patients with no or little reduction of Peg-IFN α-2b (the average dose ≥1.2 μg/kg/week) during the first 12 weeks, no significant difference was found in the relapse rate between those whose average dose of Peg-IFN α-2b was reduced to 0.6–1.2 μg/kg/week during 12–48 weeks (17%, 7/41) and those without reduction of Peg-IFN α-2b (average dose ≥1.2 μg/kg/week) (18%, 53/295) (P = 0.86) (Table 4a). Reducing the dose of Peg-IFN α-2b after week 12 in patients in whom HCV RNA had already become undetectable before week 12 did not appear to adversely influence virologic relapse when the average dose of Peg-IFN α-2b was more than 0.6 μg/kg/week during 12–48 weeks, irrespective of the mean dose of Peg-IFN α-2b during the first 12 weeks. On the other hand, the ribavirin dose reduction after week 12 tended to affect the relapse rate in patients given ≥10 mg/kg/day of the ribavirin dose during the first 12 weeks (Table 4b).

Impact of drug exposure during 0–48 weeks on relapse among VR patients with advanced fibrosis

In the evaluation of the 39 patients with VR with progression of fibrosis or cirrhosis (METAVIR fibrosis score 3 or 4) enrolled in this study, ribavirin exposure during treatment significantly correlated with relapse (nonrelapser, 10.5 ± 2.1 mg/kg/day *vs* relapser, 8.8 ± 2.3 mg/kg/day; P = 0.007). Among patients with advanced fibrosis (score 3–4), the relapse rate in patients given ≥10 mg/kg/day of the average ribavirin dose was significantly low (36%, 9/25) in comparison with that in patients given <10 mg/kg/day of ribavirin (71%, 10/14) (P = 0.048).

DISCUSSION

Previous studies have suggested that reducing the ribavirin dose within the first 12–20 weeks of treatment in patients with HCV genotype 1 was associated with a decline of SVR [7,13,14]. However, Shiffman *et al.* [8] recently reported that reducing the mean dose of ribavirin during the first 20 weeks of treatment had little impact on relapse for patients with CH-C genotype 1 and that SVR may not be adversely affected as long as the total cumulative ribavirin dose remains above 60%. As the reason for the inconsistency in the impact of reducing ribavirin on the antiviral effect, it was suggested that sample sizes of the previous studies were insufficient to assess the impact of reducing the dose of ribavirin independent of Peg-IFN. However, in Shiffman's study, while the impact of reducing the dose of Peg-IFN or ribavirin on SVR was indeed closely examined independently of each other with a large sample size, the subjects were limited to patients with advanced fibrosis or cirrhosis and prior nonresponse to Peg-IFN ± ribavirin who were enrolled in the Hepatitis Antiviral Long-term Treatment Against Cirrhosis (HALT-C) trial. Reddy *et al.* [15] analysed the drug exposure retrospectively for 569 CH-C patients with genotype 1 enrolled in clinical trials of Peg-IFN α-2a plus

Table 4 Relapse rate according to drug doses during week 0–12 and 12–48 for patients with c-EVR who completed 48 weeks of treatment

(a) Peg-IFN

Peg-IFN dose (mean, μg/kg/week)		12–48 weeks ≥1.2	0.9–1.2	0.6–0.9	<0.6
0–12 weeks	≥1.2	18% (53/295)	17% (5/30)	18% (2/11)	(1/1)
	0.9–1.2	–	22% (4/18)	33% (4/12)	60% (3/5)
	<0.9	(0/1)	(0/1)	17% (2/12)	20% (1/5)
Total*		18% (53/296)	18% (9/49)	23% (8/35)	45% (5/11)

(b) Ribavirin

Ribavirin dose (mean, mg/kg/day)		12–48 weeks ≥12	10–12	8–10	<8
0–12 weeks	≥12	4% (2/47)	13% (3/23)	13% (1/8)	33% (1/3)
	10–12	–	15% (18/123)	22% (12/54)	20% (5/25)
	8–10	–	(1/1)	26% (10/38)	26% (10/39)
	<8	–	–	–	40% (12/30)
Total†		4% (2/47)	15% (22/147)	23% (23/100)	29% (28/97)

c-EVR, complete early virologic response; Peg-IFN, pegylated interferon.
*$P = 0.18$ for comparison of the four Peg-IFN groups. †$P < 0.0001$ for comparison of the four ribavirin groups.

ribavirin, and concluded that SVR was not affected adversely by ribavirin reduction unless the cumulative ribavirin exposure was less than 60%. This supported Shiffman's data, but in Reddy's study, the stepwise reduction in ribavirin dose was shown to be associated with a stepwise increase in relapse rate from 19% to 54%. Thus, the impact of ribavirin drug exposure on the antiviral effect (relapse) in patients with CH-C genotype 1 remains unclear. Further examination is needed to determine whether or not ribavirin can be reduced to a certain degree without adversely affecting virologic relapse or SVR in Peg-IFN and ribavirin combination therapy for CH-C genotype 1.

In order to raise the SVR rate in patients with genotype 1, two strategies are possible: one is enhancing the virologic response of HCV RNA negativity and another is reducing relapse. In Peg-IFN plus ribavirin treatment, raising the doses of either or both drugs (dose-up strategy) is the only way to enhance the virologic response of HCV RNA negativity, but this is always accompanied by a high risk and the discontinuation rate can increase with the dose-up of drug, although the virologic response among patients completing the therapy can be improved [16,17]. Therefore, in this study, we tried to manage the drug dose to reduce relapse in virologic responders with HCV RNA negativity. Large-scale clinical trials [1,2,9–12] have revealed that adding ribavirin to IFN or Peg-IFN monotherapy for patients with CH-C reduced the relapse rate from approximately 50% to under 20%. Bronowicki *et al.* [18] examined the effect of ribavirin on CH-C genotype 1 in Peg-IFN α-2a plus ribavirin treatment by randomizing patients with HCV RNA negativity by week 24 into two groups, one continuing with ribavirin and the other receiving Peg-IFN α-2a alone after week 24. As a result, the virologic responders who stopped ribavirin treatment at week 24 were found to have a significantly higher rate of breakthroughs during therapy and higher relapse rates after therapy in comparison with those who received Peg-IFN plus ribavirin for the full treatment period (relapse rate; 42% vs. 29%, $P = 0.02$). These findings indicate that ribavirin plays a very important role in reducing relapse. However, the relationship between ribavirin dose and relapse rate has not been examined in detail. Considering that ribavirin has little influence on HCV RNA negativiation [1,2,9–12], its dose impact on the antiviral effect should be carefully examined, not for the SVR rate of all patients, but for the relapse rate of patients responding to Peg-IFN plus ribavirin, as evaluating of ribavirin by SVR including HCV RNA negativiation cannot differentiate it from the strong influence of the Peg-IFN effect, which affects HCV RNA negativiation dose-dependently [19]. Here, we examined the correlation between the average dose of drugs and the virologic relapse for patients responding to the treatment.

We performed univariate and multivariate analysis for relapse among the factors of mean administration doses of both drugs, including baseline factors and the timing of HCV RNA negativiation. We found exposure to ribavirin dose, timing of HCV RNA negativiation and the degree of liver fibrosis to be the independent factors affecting the virologic relapse in patients with VR. This indicates that management

of the ribavirin dose, which is the variable factor, unlike baseline factors, plays an important role in suppressing the virologic relapse in patients with CH-C genotype 1 treated by Peg-IFN plus ribavirin treatment. This suggests that maintaining the ribavirin dose should lower the relapse rate even in patients with advanced fibrosis who are liable to relapse. In fact, among patients with advanced fibrosis (METAVIR score 3–4), the relapse rate in those given ≥10 mg/kg/day of the average ribavirin dose was significantly lower than that in patients given <10 mg/kg/day of ribavirin (36% vs. 71%). However, the sample size was too small for subsequent analysis with stratification. Further study is needed to clarify the impact of ribavirin dose on viral relapse in patients with progression of fibrosis.

The relapse rate among patients with c-EVR showed a decline according to the increase in ribavirin dose during treatment week 0–48 and was not affected by the Peg-IFN α-2b dose when the patients were given more than 0.9 μg/kg/week of Peg-IFN α-2b. Among the patients with c-EVR, none with RVR had a relapse and all attained SVR irrespective of the dose of Peg-IFN α-2b or ribavirin. Examination of the impact of dose reduction after week 12 on relapse among patients with c-EVR showed that the ribavirin dose reduction after week 12 tended to affect the relapse rate in patients given ≥10 mg/kg/day of the ribavirin dose during the first 12 weeks, while the Peg-IFN α-2b dose after week 12 could be reduced without any increase in relapse rate in patients given more than 0.6 μg/kg/week of the average dose of Peg-IFN α-2b. On the other hand, maintaining the ribavirin did not lead to reduce the relapse rate in patients with LVR. About half relapsed even when given ≥12 mg/kg/day of the average ribavirin dose. This suggested that the relapse rate could not be reduced by management of the ribavirin dose in patients with LVR. Extended therapy should be chosen in LVR patients as shown in the previous studies [20–23].

Shiffman *et al.* [24] recently reported that maintaining the Hb level with epoetin alpha did not enhance SVR if ribavirin was started at the standard dose (800–1400 mg/day, mean dose 13.3 mg/kg/day), although discontinuance and the reduction rates of ribavirin were decreased and a higher mean dose of ribavirin was administered in comparison with those treated with Peg-IFN plus ribavirin without epoetin. If these findings apply to patients with CH-C genotype 1, this would suggest that the ribavirin dose does not need to be maintained during treatment with Peg-IFN plus ribavirin, which would not agree with our findings. However, closer examination of the Shiffman *et al.* study shows that Peg-IFN plus a higher dose of ribavirin (1000–1600 mg/day, mean dose 15.2 mg/kg/day) with epoetin was found to suppress the relapse rate and enhance SVR. These data agree with ours with respect to the point that higher doses of ribavirin are associated with a lower relapse rate. What differs is the ribavirin dose needed to suppress the relapse. This is likely to be due to ethnic differences between the subjects. In Shiffman's study, approximately 40% were African-Americans in whom the virologic response is well established as being significantly lower than those of other ethnic groups [25,26], while in our study, all subjects were Japanese. In the African-Americans treated with Peg-IFN plus standard-dose ribavirin, the relapse rate (calculated from 48% of ETR and 19% of SVR) was 60%, while 18% relapse (from 38% of ETR and 31% of SVR) occurred in those given Peg-IFN plus high-dose ribavirin. The relapse rate of patients with c-EVR in our study was 19%, which was very close to that for those with Peg-IFN plus high-dose ribavirin in Shiffman's study. Ribavirin does not have a direct antiviral action against HCV [27,28], and is considered to play an important role in accelerating HCV-infected cell clearance [29] and eradicating them completely when an immune response against infected cells is induced by IFN or Peg-IFN [30,31]. Therefore, the difference between patients who are easy or difficult to treat due to ethnic differences or differences in response to Peg-IFN can result in the need for different doses of ribavirin to suppress the relapse rate in patients with CH-C genotype 1.

In conclusion, our results have demonstrated that ribavirin is dose-dependently correlated with a relapse in patients with CH-C genotype 1 responding to Peg-IFN plus ribavirin. Maintaining a high dose (≥12 mg/kg/day) of ribavirin during the full treatment period could strongly suppress the relapse in such patients, while Peg-IFN α-2b could be reduced without affecting relapse in patients with c-EVR. This possibility should be explored in a prospective study.

ACKNOWLEDGEMENTS AND DISCLOSURES

Other institutions and participants in the Osaka Liver Forum are: Osaka General Medical Center, A Inoue; Toyonaka Municipal Hospital, M Inada; Sumitomo Hospital, A Yamada; Kinki Central Hospital of Mutual Aid Association of Public School Teachers, E Hayashi; Yao Municipal Hospital, H Fukui; Otemae Hospital, Y Doi; Itami City Hospital, T Kashihara; Ashiya Municipal Hospital, K Kiriyama; National Hospital Organization Minami Wakayama Medical Center, K Fujimoto; Saiseikai Senri Hospital, K Suzuki; Nishinomiya Municipal Central Hospital, H Ogawa; Kano General Hospital, S Kubota; Saso Hospital, M Nishiuchi; and Osaka Kaisei Hospital, N Imaizumi.

This work was supported by a Grant-in-Aid for Research on Hepatitis and BSE from Ministry of Health Labour and Welfare of Japan, and Scientific Research from the Ministry of Education, Science, and Culture of Japan.

REFERENCES

1 Manns MP, McHutchison JG, Gordon SC *et al.* Peginterferon alfa-2b plus ribavirin compared with interferon alfa-2b plus ribavirin for initial treatment of chronic hepatitis C: a randomised trial. *Lancet* 2001; 358: 958–965.

2 Fried MW, Shiffman ML, Reddy KR *et al.* Peginterferon alfa-2a plus ribavirin for chronic hepatitis C virus infection. *N Engl J Med* 2002; 347: 975–982.

3 Hadziyannis SJ, Sette Jr H, Morgan TR *et al.* Peginterferon-alpha2a and ribavirin combination therapy in chronic hepatitis C: a randomized study of treatment duration and ribavirin dose. *Ann Intern Med* 2004; 140: 346–355.
4 Hayashi N, Takehara T. Antiviral therapy for chronic hepatitis C: past, present, and future. *J Gastroenterol* 2006; 41: 17–27.
5 Zeuzem S, Hultcrantz R, Bourliere M *et al.* Peginterferon alfa-2b plus ribavirin for treatment of chronic hepatitis C in previously untreated patients infected with HCV genotypes 2 or 3. *J Hepatol* 2004; 40: 993–999.
6 Ferenci P, Brunner H, Laferl H *et al.* A randomized, prospective trial of ribavirin 400 mg day-1 versus 800 mg day-1 in combination with peginterferon alfa-2a in hepatitis C virus genotypes 2 and 3. *Hepatology* 2008; 47: 1816–1823.
7 McHutchison JG, Manns M, Patel K *et al.* Adherence to combination therapy enhances sustained response in genotype-1-infected patients with chronic hepatitis C. *Gastroenterology* 2002; 123: 1061–1069.
8 Shiffman ML, Ghany MG, Morgan TR *et al.* Impact of reducing peginterferon alfa-2a and ribavirin dose during retreatment in patients with chronic hepatitis C. *Gastroenterology* 2007; 132: 103–112.
9 McHutchison JG, Gordon SC, Schiff ER *et al.* Interferon alfa-2b alone or in combination with ribavirin as initial treatment for chronic hepatitis C. Hepatitis Interventional Therapy Group. *N Engl J Med* 1998; 339: 1485–1492.
10 Poynard T, Marcellin P, Lee SS *et al.* Randomised trial of interferon alpha2b plus ribavirin for 48 weeks or for 24 weeks versus interferon alpha2b plus placebo for 48 weeks for treatment of chronic infection with hepatitis C virus. International Hepatitis Interventional Therapy Group (IHIT). *Lancet* 1998; 352: 1426–1432.
11 Davis GL, Esteban-Mur R, Rustgi V *et al.* Interferon alfa-2b alone or in combination with ribavirin for the treatment of relapse of chronic hepatitis C. International Hepatitis Interventional Therapy Group. *N Engl J Med* 1998; 339: 1493–1499.
12 Lindsay KL, Trepo C, Heintges T *et al.* A randomized, double-blind trial comparing pegylated interferon alfa-2b to interferon alfa-2b as initial treatment for chronic hepatitis C. *Hepatology* 2001; 34: 395–403.
13 Davis GL, Wong JB, McHutchison JG, Manns MP, Harvey J, Albrecht J. Early virologic response to treatment with peginterferon alfa-2b plus ribavirin in patients with chronic hepatitis C. *Hepatology* 2003; 38: 645–652.
14 Shiffman ML, Di Bisceglie AM, Lindsay KL *et al.* Peginterferon alfa-2a and ribavirin in patients with chronic hepatitis C who have failed prior treatment. *Gastroenterology* 2004; 126: 1015–1023.
15 Reddy KR, Shiffman ML, Morgan TR *et al.* Impact of ribavirin dose reductions in hepatitis C virus genotype 1 patients completing peginterferon alfa-2a/ribavirin treatment. *Clin Gastroenterol Hepatol* 2007; 5: 124–129.
16 Lodato F, Azzaroli F, Brillanti S *et al.* Higher doses of peginterferon alpha-2b administered twice weekly improve sustained virological response in difficult-to-treat patients with chronic hepatitis C: results of a pilot randomized study. *J Viral Hepat* 2005; 12: 536–542.
17 Lindahl K, Stahle L, Bruchfeld A, Schvarcz R. High-dose ribavirin in combination with standard dose peginterferon for treatment of patients with chronic hepatitis C. *Hepatology* 2005; 41: 275–279.
18 Bronowicki JP, Ouzan D, Asselah T *et al.* Effect of ribavirin in genotype 1 patients with hepatitis C responding to pegylated interferon alfa-2a plus ribavirin. *Gastroenterology* 2006; 131: 1040–1048.
19 Oze T, Hiramatsu N, Yakushijin T *et al.* Peginterferon alfa-2b affects early virologic response dose-dependently in patients with chronic hepatitis C genotype 1 during treatment with pegylated interferon alfa-2b plus ribavirin. *J Viral Hepat*, in press.
20 Berg T, von Wagner M, Nasser S *et al.* Extended treatment duration for hepatitis C virus type 1: comparing 48 versus 72 weeks of peginterferon-alfa-2a plus ribavirin. *Gastroenterology* 2006; 130: 1086–1097.
21 Sanchez-Tapias JM, Diago M, Escartin P *et al.* Peginterferon-alfa2a plus ribavirin for 48 versus 72 weeks in patients with detectable hepatitis C virus RNA at week 4 of treatment. *Gastroenterology* 2006; 131: 451–460.
22 Pearlman BL, Ehleben C, Saifee S. Treatment extension to 72 weeks of peginterferon and ribavirin in hepatitis c genotype 1-infected slow responders. *Hepatology* 2007; 46(6): 1688–1694.
23 Mangia A, Minerva N, Bacca D *et al.* Individualized treatment duration for hepatitis C genotype 1 patients: a randomized controlled trial. *Hepatology* 2008; 47: 43–50.
24 Shiffman ML, Salvatore J, Hubbard S *et al.* Treatment of chronic hepatitis C virus genotype 1 with peginterferon, ribavirin, and epoetin alpha. *Hepatology* 2007; 46: 371–379.
25 Layden-Almer JE, Ribeiro RM, Wiley T, Perelson AS, Layden TJ. Viral dynamics and response differences in HCV-infected African American and white patients treated with IFN and ribavirin. *Hepatology* 2003; 37: 1343–1350.
26 Jacobson IM, Brown RS Jr, McCone J *et al.* Impact of weight-based ribavirin with peginterferon alfa-2b in African Americans with hepatitis C virus genotype 1. *Hepatology* 2007; 46: 982–990.
27 Reichard O, Andersson J, Schvarcz R, Weiland O. Ribavirin treatment for chronic hepatitis C. *Lancet* 1991; 337: 1058–1061.
28 Di Bisceglie AM, Shindo M, Fong TL *et al.* A pilot study of ribavirin therapy for chronic hepatitis C. *Hepatology* 1992; 16: 649–654.
29 Hiramatsu N, Hayashi N, Haruna Y *et al.* Immunohistochemical detection of hepatitis C virus-infected hepatocytes in chronic liver disease with monoclonal antibodies to core, envelope and NS3 regions of the hepatitis C virus genome. *Hepatology* 1992; 16: 306–311.
30 Miyatake H, Kanto T, Inoue M *et al.* Impaired ability of interferon-alpha-primed dendritic cells to stimulate Th1-type CD4 T-cell response in chronic hepatitis C virus infection. *J Viral Hepat* 2007; 14: 404–412.
31 Itose I, Kanto T, Inoue M *et al.* Involvement of dendritic cell frequency and function in virological relapse in pegylated interferon-alpha and ribavirin therapy for chronic hepatitis C patients. *J Med Virol* 2007; 79: 511–521.

J Gastroenterol (2009) 44:864–870
DOI 10.1007/s00535-009-0076-0

ORIGINAL ARTICLE—LIVER, PANCREAS, AND BILIARY TRACT

Lamivudine-to-entecavir switching treatment in type B chronic hepatitis patients without evidence of lamivudine resistance

Nao Kurashige · Kazuyoshi Ohkawa · Naoki Hiramatsu · Takayuki Yakushijin · Kiyoshi Mochizuki · Tsugiko Oze · Shinichi Kiso · Tatsuya Kanto · Tetsuo Takehara · Akinori Kasahara · Yoshinori Doi · Akira Yamada · Kazuto Fukuda · Masahide Oshita · Eiji Mita · Hiroyuki Fukui · Toshihiko Nagase · Harumasa Yoshihara · Yasuharu Imai · Michio Kato · Takeshi Kashihara · Norio Hayashi

Received: 17 February 2009 / Accepted: 15 April 2009 / Published online: 28 May 2009

Abstract
Purpose A considerable number of chronic hepatitis B (CH-B) patients remain under continuous lamivudine treatment, although switching treatment to entecavir could be beneficial. We investigated the antiviral efficacy of switching treatment to entecavir in CH-B patients without apparent evidence of lamivudine resistance during the preceding lamivudine treatment.
Methods Forty-four CH-B patients, who underwent lamivudine treatment for more than 6 months and showed no evidence of lamivudine resistance, switched to entecavir. Serial changes in hepatitis B virus (HBV) DNA were correlated with the patients' baseline HBV DNA at the commencement of entecavir administration. The entecavir-resistant substitution was examined by PCR-direct sequencing. The median follow-up period of entecavir treatment was 20 (10–23) months.
Results All 31 patients with baseline HBV DNA <2.6 logcopies/ml maintained HBV DNA-negative status during entecavir treatment. Of seven patients having HBV DNA of 2.6–<4.0 logcopies/ml, all achieved undetectable HBV DNA at the end of follow-up. As for six patients having HBV DNA ≥4.0 logcopies/ml, three patients achieved undetectable HBV DNA, whereas virological breakthrough was observed in one patient at month 15. An entecavir-resistant virus having rtM204V, rtL180M and rtS202G substitutions was detected in this patient.
Conclusions The lamivudine-to-entecavir switching treatment may be generally recommendable in CH-B patients without evidence of lamivudine resistance during

N. Kurashige · K. Ohkawa · N. Hiramatsu · T. Yakushijin · K. Mochizuki · T. Oze · S. Kiso · T. Kanto · T. Takehara · A. Kasahara · N. Hayashi (✉)
Department of Gastroenterology and Hepatology, Osaka University Graduate School of Medicine, Suita 565-0871, Japan
e-mail: hayashin@gh.med.osaka-u.ac.jp

Y. Doi
Otemae Hospital, Osaka, Japan

A. Yamada
Sumitomo Hospital, Osaka, Japan

K. Fukuda · Y. Imai
Ikeda Municipal Hospital, Ikeda, Japan

M. Oshita
Osaka Police Hospital, Osaka, Japan

E. Mita
National Hospital Organization Osaka National Hospital, Osaka, Japan

H. Fukui
Yao Municipal Hospital, Yao, Japan

T. Nagase
Suita Municipal Hospital, Suita, Japan

H. Yoshihara
Osaka Rousai Hospital, Sakai, Japan

M. Kato
National Hospital Organization Minamiwakayama Medical Center, Tanabe, Japan

T. Kashihara
Itami City Hospital, Itami, Japan

the preceding lamivudine treatment. However, great care should be taken with respect to the emergence of entecavir-resistance, especially in patients who do not respond well to the preceding lamivudine treatment.

Keywords Chronic hepatitis B · Lamivudine resistance · Entecavir-resistance

Introduction

Nucleos(t)ide analogs have been accepted as useful agents for suppressing hepatitis B virus (HBV) replication and disease progression in patients with type B chronic hepatitis (CH-B). Lamivudine, the first approved nucleoside analog, has been shown to provide short-term benefit for CH-B patients with respect to the reduction of HBV DNA, normalization of alanine aminotransferase (ALT) and improvement of liver histology [1, 2]. However, a serious shortcoming of lamivudine is the high incidence of drug resistance during long-term treatment. The detection rate of lamivudine resistance has been reported to be 24% at 1 year and 70% at 4 years of treatment [3]. Lamivudine resistance is caused by an rtM204V/I substitution within the reverse transcriptase domain of HBV polymerase gene [4–6]. An rtL180M substitution frequently emerges as a "replication-compensatory" one with the "resistance-causative" rtM204V/I substitution [4–7]. The emergence of lamivudine-resistant mutant HBV leads to the elevation of HBV DNA ("virological breakthrough") and the subsequent increase of ALT ("breakthrough hepatitis"), resulting in disease progression. Adefovir dipivoxil and tenofovir disoproxil fumarate have been shown to be effective in both nucleos(t)ide analog-naïve and lamivudine-resistant CH-B patients [8–13].

Recently, entecavir has been demonstrated to exert antiviral efficacy in both nucleos(t)ide analog-naïve and lamivudine-refractory CH-B patients [14–16]. The frequency of entecavir-resistance has been reported to be less than 1% at 4 years of treatment in nucleos(t)ide analog-naïve CH-B patients [17]. On the other hand, in switching treatment to entecavir for lamivudine-refractory CH-B patients, most of whom developed lamivudine resistance during the preceding lamivudine therapy, the cumulative probability of entecavir-resistance has been reported to be no less than 40% at 4 years of treatment [17]. Entecavir-resistance has been shown to be established by amino acid substitution(s) at rt184, rt202 and/or rt250 along with the lamivudine-resistant rtM204V and rtL180M substitutions [18]. In the case of nucleos(t)ide analog-naïve patients, the requirement of at least three amino acid substitutions serves as a high genetic barrier to entecavir-resistance. By contrast, in the case of lamivudine-resistant patients, a lower genetic barrier results in higher incidence of entecavir-resistance because two amino acid substitutions, rtM204V and rtL180M, already exist from the preceding lamivudine treatment. The reduced susceptibility to entecavir of the lamivudine-resistant virus compared with the wild-type virus is also a reason for the higher emergence rate of entecavir-resistance in lamivudine-resistant patients than in nucleos(t)ide analog-naïve ones [19].

Although lamivudine is not currently recommended as a first-line drug for nucleos(t)ide analog-naïve CH-B, a considerable number of CH-B patients are under continuous treatment with lamivudine. In these patients, the switch to entecavir treatment could be advantageous over continuation of lamivudine treatment by offering stronger antiviral efficacy and less chance of drug resistance. With respect to the manner of emergence of entecavir-resistance, switching a patient's treatment may be more appropriate before the appearance of lamivudine resistance than after its development. However, the usefulness of lamivudine-to-entecavir switching treatment has not been assessed in CH-B patients without apparent evidence of lamivudine resistance.

This led us to investigate the antiviral efficacy and emergence of entecavir-resistance in CH-B patients who showed no evidence of lamivudine resistance during the preceding lamivudine treatment and underwent the switching treatment to entecavir.

Patients and methods

Patients

This study included 44 consecutive CH-B patients from 10 institutions in the Osaka area of Japan (Otemae Hospital, Sumitomo Hospital, Osaka Police Hospital, Suita Municipal Hospital, Yao Municipal Hospital, Osaka Rousai Hospital, Ikeda Municipal Hospital, National Hospital Organization Osaka National Hospital, Itami City Hospital and Osaka University Hospital) who underwent continuous lamivudine treatment (100 mg/day) for more than 6 months and showed no apparent evidence of lamivudine resistance. Before starting the preceding lamivudine treatment, all patients had abnormal ALT, positive hepatitis B surface antigen (HBsAg) and a detectable level of HBV DNA according to PCR-based assay (Amplicor HB Monitor, Roche Diagnostics) or branched DNA assay (Quantiplex HBV DNA, Chiron). None of them showed evidence of dual infection with hepatitis C virus or human immunodeficiency virus, or other forms of liver diseases such as alcoholic liver disorder, autoimmune hepatitis and drug-induced liver injury. The total duration of the preceding lamivudine treatment ranged from 6 to 73 (median, 14)

months. The absence of lamivudine resistance was defined by no detection of the rtM204V/I substitution as measured by the PCR–enzyme linked minisequence assay (ELMA) (Sumitomo Metal Industries) [20] for 33 patients, or by the lack of virological breakthrough as judged by more than 1 log increment in HBV DNA from the nadir for the remaining 11 patients. All of the 44 patients switched to 0.5 mg/day of entecavir administration. After the beginning of entecavir treatment, liver function tests and HBV markers were measured at 1- to 2-month intervals. When virological breakthrough was observed during follow-up, entecavir-resistance-associated mutations were examined by means of a PCR-direct sequencing method. The follow-up period of entecavir treatment ranged from 10 to 23 (median 20) months.

Baseline characteristics of the patients

At the commencement of switching treatment to entecavir, the 28 males and 16 females were aged 33–79 (median 59) years. Seventeen patients (39%) tested positive for hepatitis B e antigen (HBeAg), and antibody against HBeAg (anti-HBe) developed in all of the 27 HBeAg-negative patients. Among the 27 HBeAg-negative patients, four achieved HBeAg clearance during the preceding lamivudine treatment. HBV DNA at baseline varied among patients from <2.6 to 5.2 logcopies/ml. The baseline ALT ranged from 11 to 78 (median 25) IU/l. Regarding the liver diseases of the patients, 27 (61%) showed features of chronic hepatitis, 11 (25%) of liver cirrhosis and six (14%) of hepatocellular carcinoma (HCC) according to liver biopsy and/or abdominal imaging procedures. HBV genotype was examined for 14 patients, and all of them had HBV genotype C, the most predominant genotype in Japan. Informed consent was obtained from all patients.

Serological and virological markers of HBV

HBsAg, HBeAg and anti-HBe were determined by chemiluminescent immunoassay. HBV DNA was measured by the PCR-based method (Amplicor HBV monitor, Roche Diagnostics) whose lower detection limit is 2.6 logcopies/ml. Lamivudine-resistant rtM204V/I substitution was examined by the PCR–ELMA method (Sumitomo Metal Industries) (20), which is capable of detecting the mutant virus in a mixed viral population if it is present at more than 10% of the total population. The entecavir-resistance-associated substitutions and HBV genotype were determined by a PCR-direct sequencing method. As for oligonucleotide primers for PCR reaction, the outer primer sets were BF5 (5′-AAG AGA CAG TCA TCC TCA GG-3′, nt 3183–3202) and BR1s (5′-AAA AAG TTG CAT GGT GCT GG-3′, nt 1825–1806), and the inner primer sets were BF6 (5′-CCT CCA ATT TGT CCT GGC TA-3′, nt 350–369) and BR8 (5′-TTG CGT CAG CAA ACA CTT GG-3′, nt 1195–1176). After DNA extraction, the DNA sample was subjected to the PCR reaction for 35 cycles (denaturation at 94°C for 1 min, annealing at 55°C for 1 min and extension at 72°C for 2 min) using the inner primer set, followed by a final extension at 72°C for 10 min. If amplification was not successful by the single PCR reaction, the nested PCR was conducted; the first round PCR was done using the outer primer sets for 35 cycles, and the aliquot of the product was used for the second round PCR for 30 cycles using inner primer sets. All sequencing reactions of the PCR products were carried out using the BigDye Terminater Ver. 3.1 Cycle Sequencing Kit, and 3100 or 3730 Genetic Analyzer (Applied Biosystems), which allowed determination of the amino acid sequences of rt85-344. For determining the HBV genotype, nucleotide sequences obtained in each of the patients were aligned along with representative HBV strains of genotype A–H, and a phylogenetic tree was constructed in the homepage of DNA Data Bank of Japan (http://www.ddbj.nig.ac.jp).

Statistical analysis

Statistical analysis for group comparison was performed by Fisher's exact probability test and Mann–Whitney's non-parametric U test using the SPSS version 15.0J software (SPSS Inc, Chicago, IL). A p value of less than <.05 was considered to be significant.

Results

Classification of patients who underwent lamivudine-to-entecavir switching treatment according to baseline HBV DNA

The 44 CH-B patients who underwent the switching treatment from lamivudine to entecavir were first classified according to their baseline HBV DNA at the commencement of entecavir administration. HBV DNA was not detectable (<2.6 logcopies/ml) in 31 patients (70%) at baseline. Seven patients (16%) had baseline HBV DNA of 2.6–<4.0 logcopies/ml. In the remaining six patients (14%), the baseline HBV DNA was ≥4.0 logcopies/ml. When patient clinical characteristics were compared among the three patient groups (Table 1), nine (29%) of the 31 patients with baseline HBV DNA <2.6 copies/ml tested positive for HBeAg at the commencement of switching treatment to entecavir, compared with five of the six (83%) patients with baseline HBV DNA ≥4.0 copies/ml ($p < .05$). Gender ratio, age, ALT at baseline, liver disease, duration of the preceding lamivudine treatment and

Table 1 Patient clinical characteristics and the therapeutic efficacy in 44 CH-B patients in relation to their baseline HBV DNA

	Baseline HBV DNA		
	<2.6 logcopies/ml ($n = 31$)	2.6–<4.0 logcopies/ml ($n = 7$)	≥4.0 logcopies/ml ($n = 6$)
At the commencement of switching treatment to entecavir			
Gender (male/female)	19/12	5/2	4/2
Age (years)	60 (35–79)[a]	65 (41–69)	55 (33–65)
HBeAg (positive/negative)	9/22	3/4	5/1[b]
HBV DNA (logcopies/ml)	<2.6	3.1 (2.6–3.6)[c]	4.6 (4.0–5.2)[c,d]
rtM204V/I mutation (absence/NT)	23/8	5/2	5/1
ALT (IU/l)	25 (11–64)	31 (13–46)	20 (17–78)
Chronic hepatitis/cirrhosis/HCC	19/7/5	4/2/1	4/2/0
Follow-up period of entecavir treatment (months)	19 (10–23)	19 (10–22)	20 (16–22)
The rate of undetectable HBV DNA level during follow-up	31 (100%)	7 (100%)	3 (50%)[c]
Emergence of entecavir-resistance during follow-up	0 (0%)	0 (0%)	1 (17%)
At the commencement of preceding lamivudine treatment			
HBeAg (positive/negative)	12/19	4/3	5/1
HBV DNA (logcopies/ml)	6.5 (4.3–7.6‹)	6.6 (6.2–7.6‹)	7.6‹ (5.9–7.6‹)
Duration of preceding lamivudine treatment (months)	15 (6–73)	10 (7–42)	9 (8–32)

NT not tested

[a] Values are expressed as median (range)

[b] $p < .05$ versus baseline HBV DNA <2.6 logcopies/ml group

[c] $p < .01$ versus baseline HBV DNA <2.6 logcopies/ml group

[d] $p < .01$ versus baseline HBV DNA of 2.6–<4.0 logcopies/ml group

follow-up period of entecavir treatment did not differ among the three groups. Also, there was no significant difference in HBV DNA and the frequency of positive HBeAg at the commencement of preceding lamivudine treatment among them.

Antiviral efficacy and drug resistance in lamivudine-to-entecavir switching treatment in relation to baseline HBV DNA

Next, we investigated serial changes in HBV DNA after the switch from lamivudine to entecavir treatment in CH-B patients in relation to the baseline HBV DNA. All 31 patients with baseline HBV DNA <2.6 logcopies/ml maintained undetectable HBV DNA during the follow-up period of entecavir treatment. Figure 1 shows the longitudinal evaluation of HBV DNA during the switching treatment to entecavir in patients with a detectable level of baseline HBV DNA. In patients having baseline HBV DNA of 2.6–<4.0 logcopies/ml (Fig. 1a), all of the seven patients achieved sustained undetectable HBV DNA during follow-up, although HBV DNA was transiently detected in one patient. As for patients having baseline HBV DNA ≥4.0 logcopies/ml (Fig. 1b), three (50%) of the six patients achieved sustained undetectable HBV DNA during follow-up. In two patients, HBV DNA was not cleared entirely, but declined to 2.9 and 2.7 logcopies/ml at month 18, respectively. In sequencing analysis at that time, the former patient had the lamivudine-resistant rtM204I substitution, although it was not detected by the PCR–ELMA assay at the start of entecavir treatment. The latter patient had no drug resistance-associated substitutions. In the sixth patient, HBV DNA decreased initially, but virological breakthrough was seen at month 15. The entecavir-resistant virus was detected after virological breakthrough. The detailed disease course of the entecavir-resistant patient is described below. As for the relationship of baseline HBV DNA to the frequency of undetectable HBV DNA, HBV DNA was cleared more frequently in patients with baseline HBV DNA <2.6 logcopies/ml than in those with baseline HBV DNA ≥4.0 logcopies/ml (100 vs. 50%, $p < .01$) (Table 1).

Serial changes in ALT during lamivudine-to-entecavir switching treatment were further examined. Among the 31 patients with baseline HBV DNA <2.6 logcopies/ml, the baseline ALT was within the normal range (≤40 IU/l) in 27 patients, 24 of whom showed sustained ALT normalization during follow-up. In the remaining three patients, ALT became slightly abnormal (≤60 IU/l) during follow-up. As for four patients with abnormal baseline ALT, the level was normalized in three, whereas a slight elevation of ALT (≤60 IU/l) continued in one during follow-up.

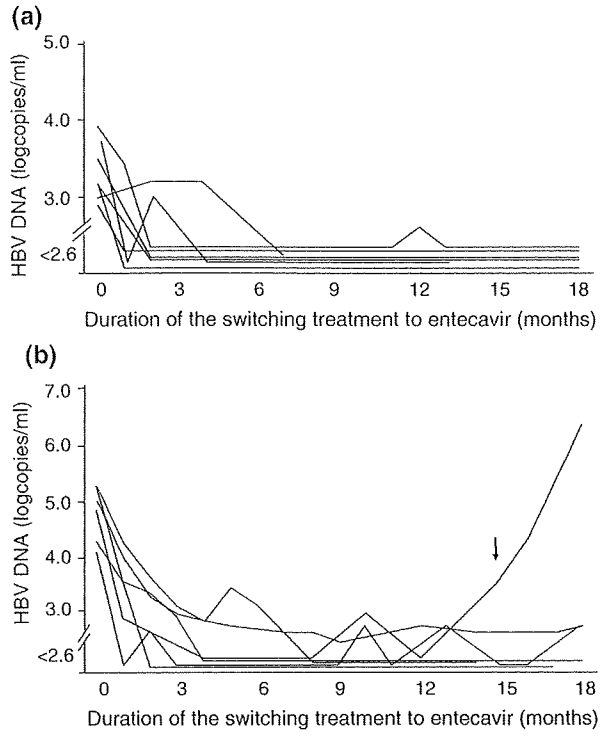

Fig. 1 Changes in HBV DNA after commencement of switching treatment from lamivudine to entecavir in CH-B patients with baseline HBV of (**a**) 2.6–<4.0 logcopies/ml and (**b**) ≥4.0 logcopies/ml. The *black arrow* indicates the time point of virological breakthrough

Among the 13 patients having a detectable level of baseline HBV DNA, five patients (three with baseline HBV DNA of 2.6–<4.0 logcopies/ml and two with baseline HBV DNA ≥4.0 logcopies/ml) had abnormal ALT at baseline but showed ALT normalization during follow-up. In the remaining eight patients, ALT continued to be normal from the beginning of entecavir treatment.

Disease course of the CH-B patients showing entecavir-resistance during lamivudine-to-entecavir switching treatment

The disease course of the entecavir-resistant patient is shown in Fig. 2. This patient was a 33-year-old HBeAg-positive male, whose liver biopsy showed features of chronic hepatitis. He underwent the preceding lamivudine treatment for 8 months. HBV DNA decreased from >7.6 to 4.6 logcopies/ml, and ALT was normalized during the lamivudine therapy. The rtM204V/I substitution was not detected before the switch to entecavir treatment by the PCR–ELMA analysis. After the commencement of entecavir treatment, HBV DNA was cleared at month 5. However, virological breakthrough was seen at month 15, and HBV DNA was further increased to 6.1 logcopies/ml at month 18. The sequencing analysis at month 18 revealed the rtM204V, rtL180M and rtS202G substitutions. Two additional substitutions, rtL267M and rtQ316H, were also found, when the amino acid sequences were compared with three representative genotype C HBV isolates (Genbank accession nos. V00867, X01587 and D00630) [21–23]. Breakthrough hepatitis was not evident after the emergence of entecavir-resistant mutant virus. The sequencing analysis also revealed that he was infected with HBV of genotype C.

Discussion

Entecavir treatment has been shown to exhibit more powerful antiviral efficacy and less frequent drug resistance than lamivudine treatment in nucleos(t)ide analog-naïve CH-B patients [14, 15, 17]. Entecavir is also effective in patients showing lamivudine resistance during the preceding lamivudine treatment, but its efficacy is limited due to the higher incidence of entecavir-resistance, compared with nucleos(t)ide analog-naïve ones [16, 17]. This is because entecavir-resistance is established based on two lamivudine-resistant substitutions, rtM204V and rtL180M, and additional mutation(s) occurring at rt184, rt202 and/or rt250 [18]. A considerable number of CH-B patients remain under continuous lamivudine treatment, while the lamivudine-to-entecavir switching treatment could yield a practical benefit. The switching treatment may be more promising for patients before the appearance of lamivudine resistance than after its development. In the present study, we investigated the efficacy of lamivudine-to-entecavir switching treatment in CH-B patients without apparent evidence of lamivudine resistance during the preceding lamivudine treatment.

We evaluated the antiviral efficacy of the switching treatment to entecavir in relation to the baseline HBV DNA at the commencement of the entecavir administration. In all patients having baseline HBV DNA <2.6 logcopies/ml, who revealed a good response to the preceding lamivudine treatment, HBV DNA continued to be undetectable during the switching treatment to entecavir. Also, all patients having baseline HBV DNA of 2.6–<4.0 logcopies/ml achieved sustained undetectable HBV DNA during the follow-up period of entecavir treatment. Among six patients having baseline HBV DNA ≥4.0 logcopies/ml, who did not respond well to the preceding lamivudine treatment, HBV DNA was cleared in three during follow-up. Its reduction by up to 3.0 logcopies/ml was seen in two additional cases without emergence of the entecavir-resistant virus. Thus, the antiviral efficacy of the lamivudine-to-entecavir switching treatment was exhibited in almost all CH-B patients in parallel with that of the preceding

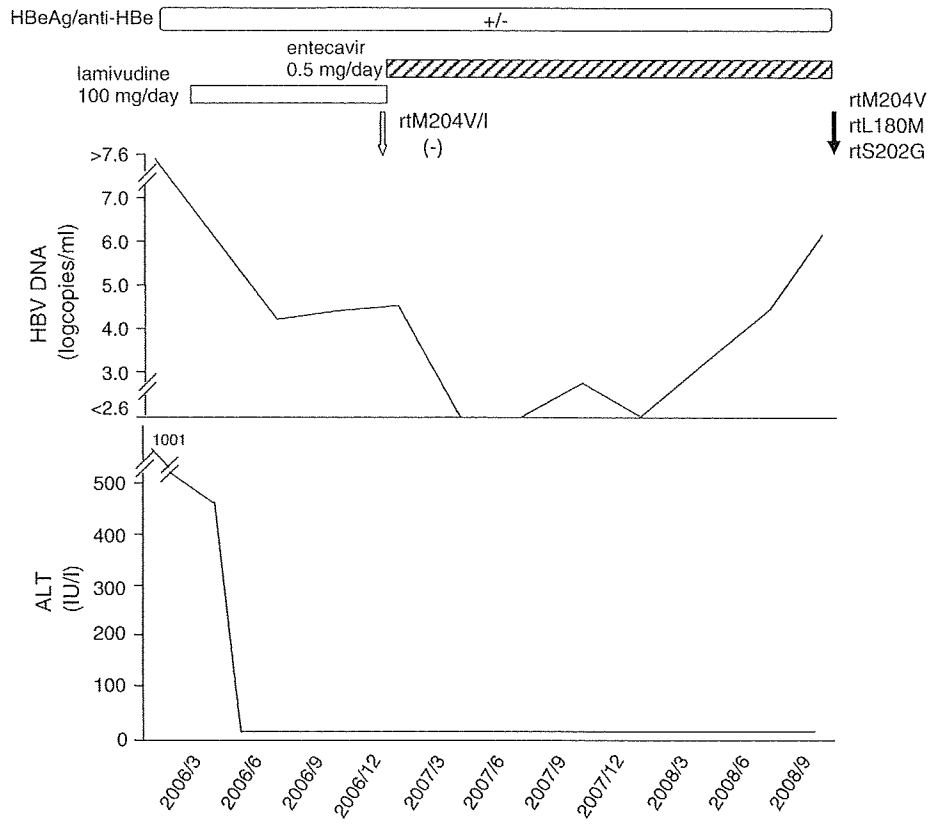

Fig. 2 Disease course of the CH-B patient showing entecavir-resistance during switching treatment to entecavir. The *white arrow* indicates the time point of the PCR–ELMA assay to detect rtM204V/I mutation, whereas the *black arrow* indicates the time point of the PCR-direct sequencing analysis

lamivudine treatment. In addition, the switching treatment to entecavir tended to yield a greater decrease in HBV DNA than the preceding lamivudine treatment. These results indicate that the switch from lamivudine to entecavir may be generally recommendable compared with continuation of lamivudine administration in CH-B patients without evidence of lamivudine resistance.

In this study, one of the six patients having baseline HBV DNA $\geq$4.0 logcopies/ml showed entecavir-resistance during the switching treatment to entecavir. It was probably due to the existence of an extremely small amount of lamivudine-resistant virus mixed with a predominant wild-type virus, which could not be detected by the sensitive PCR–ELMA assay at the start of the switch to entecavir treatment. It is speculated that, during entecavir treatment, the lamivudine-resistant virus having rtM204V and rtL180M substitutions may become predominant with time, followed by the establishment of entecavir-resistant virus via the additional rtS202G substitution. Compared to the low incidence of drug resistance in entecavir treatment for nucleos(t)ide analog-naïve CH-B patients [17], the entecavir-resistance may occur more frequently in the lamivudine-to-entecavir switching treatment for patients without evidence of lamivudine resistance. In particular, patients who do not achieve a good response to the preceding lamivudine treatment are speculated to have a higher risk for the development of entecavir-resistance in the switching treatment to entecavir, although it should be verified by further studies.

In conclusion, in CH-B patients receiving the continuous lamivudine treatment, it may be recommendable to switch to entecavir treatment before the appearance of lamivudine resistance. It may contribute to reducing the subsequent emergence of drug resistance. However, great care should be taken with respect to the emergence of entecavir-resistant virus after the switch to entecavir treatment, especially in patients who do not respond well to the preceding lamivudine treatment. Our retrospective study with a small number of patients and a short duration of follow-up cannot draw a definite conclusion but still provides some information about the clinical possibilities of the lamivudine-to-entecavir switching treatment. Further detailed investigation with a larger number of patients and a longer follow-up period may offer better understanding.

References

1. Lai CL, Chien RN, Leung NW, Chang TT, Guan R, Tai DI, et al. A one-year trial of lamivudine for chronic hepatitis B. Asia Hepatitis Lamivudine Study Group. N Engl J Med. 1998;339:61–8.
2. Dienstag JL, Schiff ER, Wright TL, Perrillo RP, Hann HW, Goodman Z, et al. Lamivudine as initial treatment for chronic

hepatitis B in the United States. N Engl J Med. 1999;341:1256–63.
3. Lai CL, Dienstag J, Schiff E, Leung NW, Atkins M, Hunt C, et al. Prevalence and clinical correlates of YMDD variants during lamivudine therapy for patients with chronic hepatitis B. Clin Infect Dis. 2003;36:687–96.
4. Allen MI, Deslauriers M, Andrews CW, Tipples GA, Walters KA, Tyrrell DL, et al. Identification and characterization of mutations in hepatitis B virus resistant to lamivudine. Lamivudine Clinical Investigation Group. Hepatology. 1998;27:1670–7.
5. Liaw YF, Chien RN, Yeh CT, Tsai SL, Chu CM. Acute exacerbation and hepatitis B virus clearance after emergence of YMDD motif mutation during lamivudine therapy. Hepatology. 1999;30:567–72.
6. Westland CE, Yang H, Delaney WE 4th, Wulfsohn M, Lama N, Gibbs CS, et al. Activity of adefovir dipivoxil against all patterns of lamivudine-resistant hepatitis B viruses in patients. J Viral Hepat. 2005;12:67–73.
7. Ono-Nita SK, Kato N, Shiratori Y, Lan KH, Yoshida H, Carrilho FJ, et al. Susceptibility of lamivudine-resistant hepatitis B virus to other reverse transcriptase inhibitors. J Clin Invest. 1999; 103:1635–40.
8. Hadziyannis SJ, Tassopoulos NC, Heathcote EJ, Chang TT, Kitis G, Rizzetto M, et al. Adefovir dipivoxil for the treatment of hepatitis B e antigen-negative chronic hepatitis B. N Engl J Med. 2003;348:800–7.
9. Marcellin P, Chang TT, Lim SG, Tong MJ, Sievert W, Shiffman ML, et al. Adefovir dipivoxil for the treatment of hepatitis B e antigen-positive chronic hepatitis B. N Engl J Med. 2003; 348:808–16.
10. Perrillo R, Hann HW, Mutimer D, Willems B, Leung N, Lee WM, et al. Adefovir dipivoxil added to ongoing lamivudine in chronic hepatitis B with YMDD mutant hepatitis B virus. Gastroenterology. 2004;126:81–90.
11. Peters MG, Hann Hw H, Martin P, Heathcote EJ, Buggisch P, Rubin R, et al. Adefovir dipivoxil alone or in combination with lamivudine in patients with lamivudine-resistant chronic hepatitis B. Gastroenterology. 2004;126:91–101.
12. van Bömmel F, Wünsche T, Mauss S, Reinke P, Bergk A, Schürmann D, et al. Comparison of adefovir and tenofovir in the treatment of lamivudine-resistant hepatitis B virus infection. Hepatology. 2004;40:1421–5.
13. van Bömmel F, Zöllner B, Sarrazin C, Spengler U, Hüppe D, Möller B, et al. Tenofovir for patients with lamivudine-resistant hepatitis B virus (HBV) infection and high HBV DNA level during adefovir therapy. Hepatology. 2006;44:318–25.
14. Chang TT, Gish RG, de Man R, Gadano A, Sollano J, Chao YC, et al. A comparison of entecavir and lamivudine for HBeAg-positive chronic hepatitis B. N Engl J Med. 2006;354:1001–10.
15. Lai CL, Shouval D, Lok AS, Chang TT, Cheinquer H, Goodman Z, et al. Entecavir versus lamivudine for patients with HBeAg-negative chronic hepatitis B. N Engl J Med. 2006;354:1011–20.
16. Sherman M, Yurdaydin C, Sollano J, Silva M, Liaw YF, Cianciara J, et al. Entecavir for treatment of lamivudine-refractory, HBeAg-positive chronic hepatitis B. Gastroenterology. 2006;130:2039–49.
17. Colonno RJ, Rose R, Pokornowski K, Baldick C, Eggers B, Yu D, et al. Four year assessment of ETV resistance in nucleoside-naïve and lamivudine refractory patients. J Hepatol. 2007; 46:S294. (Abst.).
18. Tenney DJ, Rose RE, Baldick CJ, Levine SM, Pokornowski KA, Walsh AW, et al. Two-year assessment of entecavir resistance in Lamivudine-refractory hepatitis B virus patients reveals different clinical outcomes depending on the resistance substitutions present. Antimicrob Agents Chemother. 2007;51:902–11.
19. Levine S, Hernandez D, Yamanaka G, Zhang S, Rose R, Weinheimer S, et al. Efficacies of entecavir against lamivudine-resistant hepatitis B virus replication and recombinant polymerases in vitro. Antimicrob Agents Chemother. 2002;46:2525–32.
20. Kobayashi S, Ide T, Sata M. Detection of YMDD motif mutations in some lamivudine-untreated asymptomatic hepatitis B virus carriers. J Hepatol. 2001;34:584–6.
21. Ono Y, Onda H, Sasada R, Igarashi K, Sugino Y, Nishioka K. The complete nucleotide sequences of the cloned hepatitis B virus DNA; subtype adr and adw. Nucleic Acids Res. 1983; 11:1747–57.
22. Fujiyama A, Miyanohara A, Nozaki C, Toneyama T, Ohtomo N, Matsubara K. Cloning and structural analyses of hepatitis B DNAs, subtype *adr*. Nucleic Acids Res. 1983;11:4601–10.
23. Kobayashi M, Koike K. Complete nucleotide sequence of hepatitis B virus DNA of subtype adr and its conserved gene organization. Gene. 1984;30:227–32.

BioSystems 99 (2010) 70–78

Contents lists available at ScienceDirect

BioSystems

journal homepage: www.elsevier.com/locate/biosystems

Reproducibility and usability of chronic virus infection model using agent-based simulation; comparing with a mathematical model

Jun Itakura[a,*], Masayuki Kurosaki[a], Yoshie Itakura[a], Sinya Maekawa[b], Yasuhiro Asahina[a], Namiki Izumi[a], Nobuyuki Enomoto[b]

[a] Division of Gastroenterology and Hepatology, Musashino Red Cross Hospital, 1-26-1 Kyonan-cho, Musashino-shi, Tokyo 180-8610, Japan
[b] First Department of Internal Medicine, Faculty of Medicine, University of Yamanashi, 1110, Shimogatou, Chuou-shi, Yamanashi 409-3898, Japan

ARTICLE INFO

Article history:
Received 30 June 2009
Received in revised form 27 August 2009
Accepted 6 September 2009

Keywords:
Agent-based model
Virus infectious disease

ABSTRACT

We created agent-based models that visually simulate conditions of chronic viral infections using two software. The results from two models were consistent, when they have same parameters during the actual simulation. The simulation results comprise a transient phase and an equilibrium phase, and unlike the mathematical model, virus count transit smoothly to the equilibrium phase without overshooting which correlates with actual biology in vivo of certain viruses. We investigated the effects caused by varying all the parameters included in concept; increasing virus lifespan, uninfected cell lifespan, uninfected cell regeneration rate, virus production count from infected cells, and infection rate had positive effects to the virus count during the equilibrium period, whereas increasing the latent period, the lifespan-shortening ratio for infected cells, and the cell cycle speed had negative effects. Virus count at the start did not influence the equilibrium conditions, but it influenced the infection development rate. The space size had no intrinsic effect on the equilibrium period, but virus count maximized when the virus moving speed was twice the space size. These agent-based simulation models reproducibly provide a visual representation of the disease, and enable a simulation that encompasses parameters those are difficult to account for in a mathematical model.

1. Introduction

All viruses need hosts as a basis for their life. When a virus enters the host body, it invades cells and uses both its own enzymes and those of the host cells to replicate. Host cells infected by viruses launch a self-defense system known as the innate immune system (See and Wark, 2008; Naniche, 2009), which inhibits viral replication and uses the human leukocyte antigen system and cytokines to elicit an immune response. Immune cells that have received signals from host cells activate other immune cells, neutralize viruses in the serum by means of antibodies, and prevent the virus from replicating and proliferating by destroying or curing host cells. Viral infection is a disorder based on the interactions between viruses and cells.

The power relationship between these agents changes along with the progression of the disease. In the very early stages of infection, as the host defense mechanisms are immature, the virus has the ability to overwhelm the host cells, actively replicate, and proliferate. Subsequently, as the capacity of the immune system improves, the speed of viral proliferation drops and the virus count reaches a peak. Infected host cells begin to be disrupted by the immune system or virus particles, and symptoms appear as a result. If the immune system is stronger than the virus, then the viral counts decline, and, in transient viral disorders, the virus is finally eliminated and the host recovers. In chronic viral disorders, however, the power relationship between the virus and host cells reaches equilibrium, and a long-term power balance is maintained with the virus count reaching a plateau.

Mathematical models have been proposed to study the dynamics of such viral disorders, and are regarded as being of value in understanding this phenomenon (Ho et al., 1995; Nowak et al., 1996; Neumann et al., 1998). However, these models are difficult to understand for clinicians, and their applicability is somewhat limited in everyday practice. In clinical research, measurements of viral dynamics in patients for short duration have been made for human

Abbreviations: HIV, human immunodeficiency virus; HBV, hepatitis B virus; HCV, hepatitis C virus.

* Corresponding author. Tel.: +81 422 32 3111; fax: +81 422 32 9551.
E-mail address: jitakura@musashino.jrc.or.jp (J. Itakura).

0303-2647/$ – see front matter © 2009 Elsevier Ireland Ltd. All rights reserved.
doi:10.1016/j.biosystems.2009.09.001

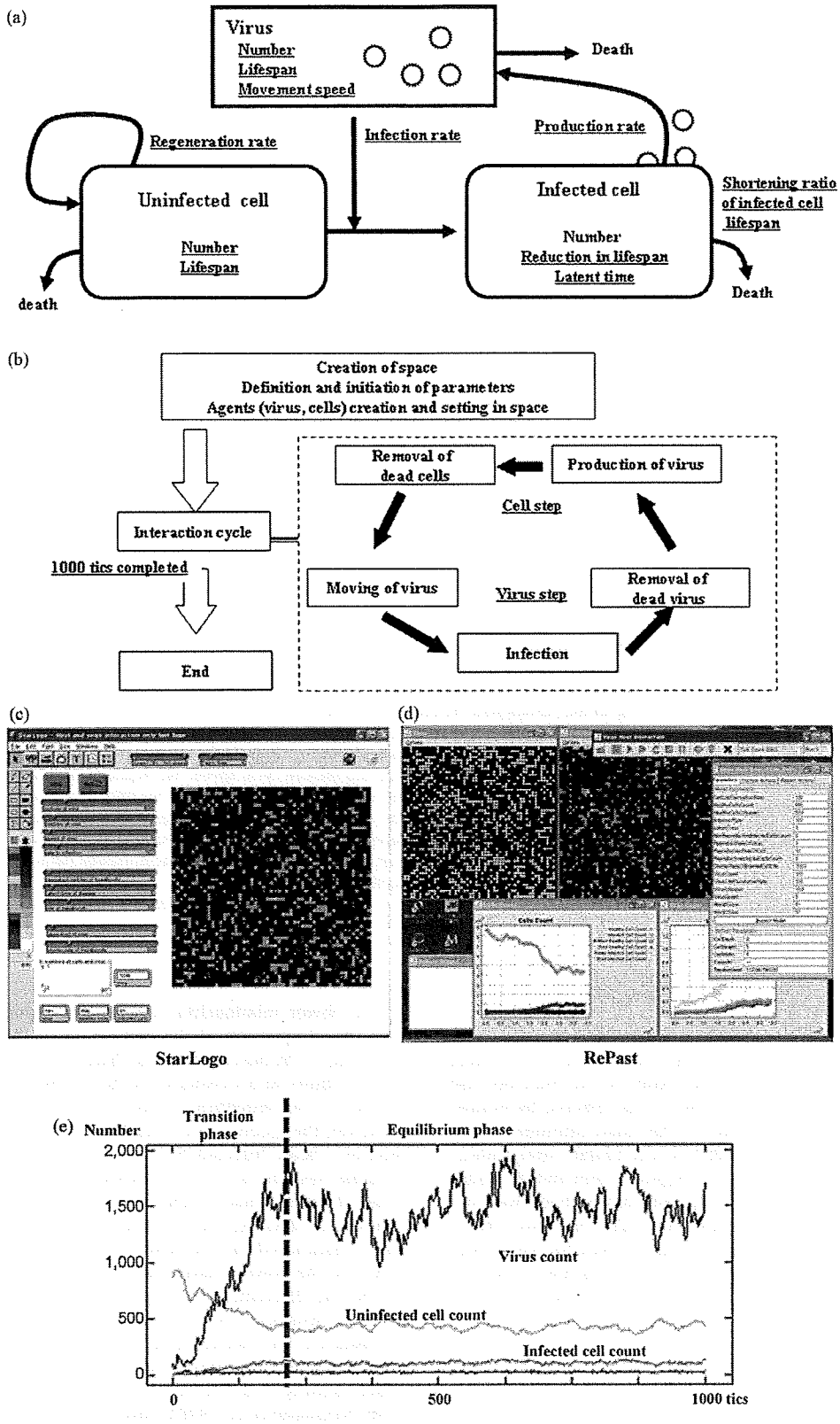

Fig. 1. Simulation design and an example of simulation results. (a) Model concept. Viruses, uninfected cells, and infected cells were treated as agents, and parameters were set for each of these and for interactions between agents (underlined). (b) Flowchart of the program. After preparing the simulation, we entered the interaction cycle, in which virus steps (such as movement) and cell steps were repeated. One cycle was counted as 1 tic, and the simulation concluded after 1000 tics. (c and d) Simulation screen using (c) StarLogo and (d) RePast. Yellow circles are viruses, green squares are uninfected cells, and orange and red indicate infected cells, with orange indicating the latent period. In StarLogo, all the agents are shown on the same screen, but in RePast, viruses and cells are shown in separate windows. (e) Example of a simulation chart in StarLogo. After the start of simulation the virus count and infected cell count increase while the uninfected cell count decreases, with equilibrium state reached after a certain number of tics.

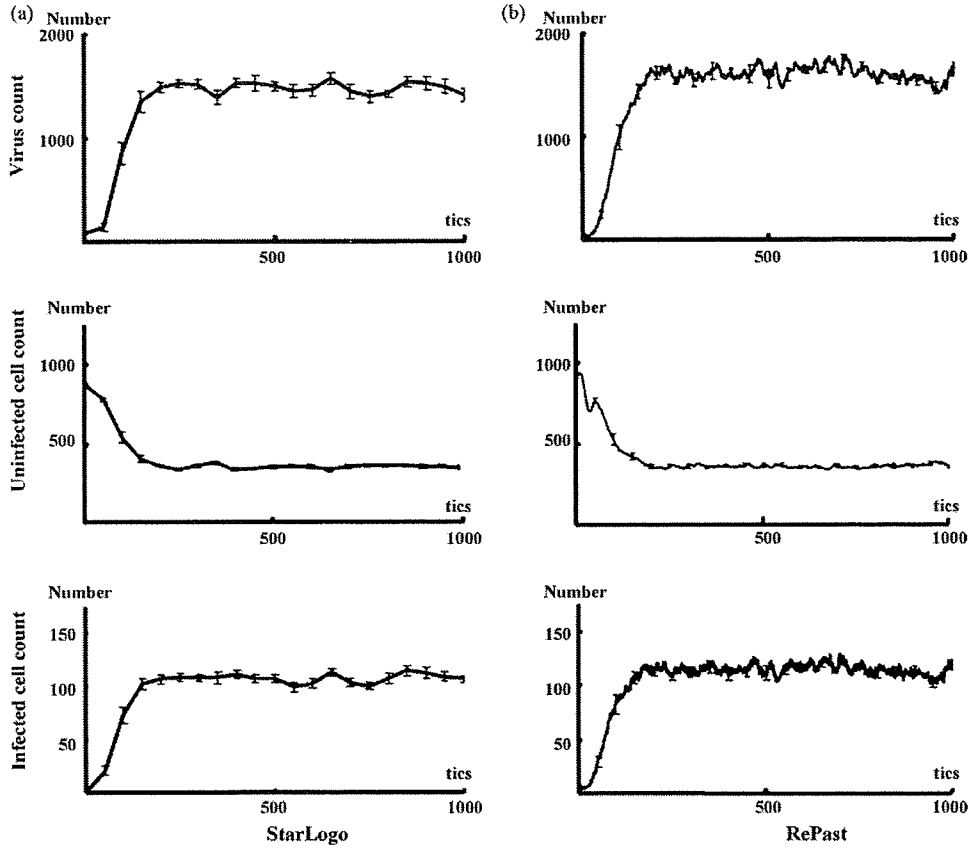

Fig. 2. Comparison of simulation results in (a) StarLogo and (b) RePast. The results were consistent when the parameters were made consistent. (Virus count [average ± SD]: StarLogo 1458.03 ± 173.1, RePast 1462.71 ± 178.8, $p = 0.94$. Uninfected cell count: 364.24 ± 30.4, 368.11 ± 33.4, $p = 0.83$. Infected cell count: 105.73 ± 13.0, 107.74 ± 13.0, $p = 0.24$. Unpaired Student's t-test.) Parameter values were set as follows: initial virus count, 100; uninfected cell count, 880; infected cell count, 0; virus speed of movement, 5 grids/tic; infection rate, 10%; uninfected cell regeneration rate, 1%; latent period, 3 tics; and virus reproduction rate, 5/cells/tic. The following parameter settings were taken from actual measurements: virus lifespan, 4.5 tics; uninfected cell lifespan, 49.8 tics; and infected cell lifespan, 6.7 tics.

immunodeficiency virus (HIV) (Ho et al., 1995), hepatitis B virus (HBV) (Nowak et al., 1996) and hepatitis C virus (HCV) (Neumann et al., 1998), and research is also underway on a range of models based on animal experiments and cell culture systems. As chronic viral disorders persist over long periods of time complete follow-up of viral dynamics is difficult. Furthermore, limitations of items that can be measured, such as the difficulty of measuring whole numbers of host cells, make it extremely difficult to investigate their consistency in mathematical models.

The recent ascend of dynamic-models owes much to advances in computers. Computer performance has improved markedly in recent years, not only in terms of their calculating capacity but also with regard to image displays, and models that offer a visual representation of viral disorders are now being reported (Gilbert and Bankes, 2002; Duca et al., 2007; Shapiro et al., 2008; Castiglione et al., 2007). One advantage of such visual models is that by providing a visual representation, they make understanding the disease status easy. Another benefit is that they enable parameters to be identified that are hidden as background noise in mathematical models. However, these models have some problems; it is difficult to prove the reproducibility of the simulation results derived from different languages or libraries, difficult to prove the validity of the model's concepts, and difficult to prove that the simulation results accurately reflect the reality. In this study, we created agent-based computer models that visually simulate the conditions of chronic viral infections using two software. The reproducibility of two agent-based computer models and the differences between agent-based models and the mathematical model were analyzed. This agent-based model enabled us to investigate how each parameter included in the concept affects the conditions of chronic viral infections.

2. Methods

2.1. Selection of Software

In this study, we used two different types of softwares: StarLogo version 2.0 (http://education.mit.edu/starlogo/) supplied by MIT Media Laboratory and Recursive Porous Agent Simulation Toolkit (RePast-3.0, http://repast.sourceforge.net/) supplied by the Argonne National Laboratory. StarLogo uses Logo, one of the simplest programming languages, and has a fixed graphical user interface. RePast is a library that uses Java, another programming language, which also has a fixed graphical user interface.

Logo is an assembly language, and StarLogo carries out processing sequentially. Java is an object-oriented language, and RePast has a faster processing speed than StarLogo. In addition, StarLogo has a number of stipulations to simplify simulations, such as parameters can only be set up to five decimal places and the simulation space is also fixed as 51×51 square grids. RePast, on the other hand, has fewer such restrictions. Thus, it offers a higher degree of freedom in program settings than StarLogo. Taking simulation space as an example, in spite of the restrictions imposed by the underlying operating system's image display system, any number of grids can be set and a hexagonal grid could also be chosen rather than a square one. However, users must stipulate and set all parameters themselves. This means that they must first declare the shape of the grid and the number of grids they will use to fill the simulation space. Java is also more difficult to learn than Logo, and debugging and correcting the program is also more difficult. Thus, it is difficult to judge whether or not the results agree with the planned simulation.

In effect, these two different types of softwares are polar opposites. It is simple to start a simulation in StarLogo, but producing results takes time and it is difficult to carry out more complex simulations. In RePast it is difficult to compose the program and judge whether or not the planned study has actually been achieved, but the

simulation itself takes only a short time to complete and there are lesser restrictions in the construction of a simulation model.

2.2. Concept for Modeling

We applied the basic virus–host interaction mathematical model to the agent-based simulation system with slight modifications. The mathematical model was used to describe the dynamics of HIV (Ho et al., 1995), HBV (Nowak et al., 1996), and HCV (Neumann et al., 1998) and the only agents involved were host cells and viruses, without the inclusion of immune cells. The effects of the immune system are expressed by varying parameters such as lifespan of host cells and viruses.

Fig. 1a illustrates the study concept. Viruses have the ability to infect healthy host cells (uninfected cells) and the infected cells produce new viruses. Both cells and viruses have definite lifespans, and the lifespan of infected cells is usually shorter than that of uninfected cells. Uninfected cells automatically regenerate within the space, whereas infected cells only arise due to infection of uninfected cells. Viruses also lack the ability to regenerate themselves and are only produced from infected cells.

2.3. Parameter Settings

In the present study, as the StarLogo settings are circumscribed, we limited the simulation space to 51 × 51 square grids. However, we made an exception here while investigating the effects of size of space on the simulation results. The numbers of viruses, uninfected cells, and infected cells could only be set before the start of the simulation. As described in the later, our simulation ran in cycles, with 1 cycle defined as 1 tic.

In mathematical simulation models, the death rate is required as a parameter. However, in our program we set lifespans for viruses and uninfected cells. These lifespans were not uniform, but were set to have a deviation of about 10%. The lifespan of cells was shortened by infection with ratio decided beforehand.

The infection ratio was meaningful only when an infected cell and a virus coincidentally occupied the same grid, and this was used to calculate the probability of the infection occurring in that situation. The virus production rate was set as the number of viruses produced by an infected cell during 1 tic. Infected cells could be set as a parameter indicating the latent period between the time of virus infection and the time of virus replication.

In order to emulate the tissue repair capacity, we set uninfected cell regeneration rate such that grids without any cells had a specified probability of producing uninfected cells on top of themselves. As a result, the more the cell count declined within a space the more regenerated uninfected cells were produced, whereas the number of regenerated cells declined as cell count increased.

The number of grids through which a virus could move in 1 tic was set as the speed of movement, and the direction of movement was set within a range of 90° toward the top of the simulation space. The program used a circulatory method of movement; when a virus arrived at the top of the space, it was translocated to the bottom, and moved again toward the top. Cells were fixed on the grid.

2.4. Simulation Flowchart

Fig. 1b shows a flowchart of the program. First, the simulation space was produced, after which each parameter was defined and the initial settings were made. Next the agents – viruses and uninfected and infected cells – were produced. The simulation cycle was as follows. Viruses moved to a new grid, and if an uninfected cell was present, this was infected with a probability based on the infection rate. The lifespan of the virus decreased, and viruses that had completed their lifespan and those that had caused an infection were removed from the space. Infected cells produced new viruses, the lifespans of both uninfected and infected cells decreased. Then, cells that had completed their lifespan were eliminated and a new cycle began. The program was set such that the simulation ended after this cycle had repeated 1000 times. This meant that one simulation was complete after 1000 tics.

2.5. Data Collection

The RePast model was programmed such that data for each tic was saved automatically as a text file at the end of the simulation. This text file could be opened by a database software. The StarLogo model was programmed to stop the simulation and collect data after every 50 tics.

2.6. Mathematical Model

In order to compare the results of this agent-based simulation, we used a viral infection mathematical model, which we improved as follows.

$$\frac{dT}{dt} = s[2601 - (T + I)] - dT - bVT \quad (1)$$

$$\frac{dI}{dt} = bVT - dI \quad (2)$$

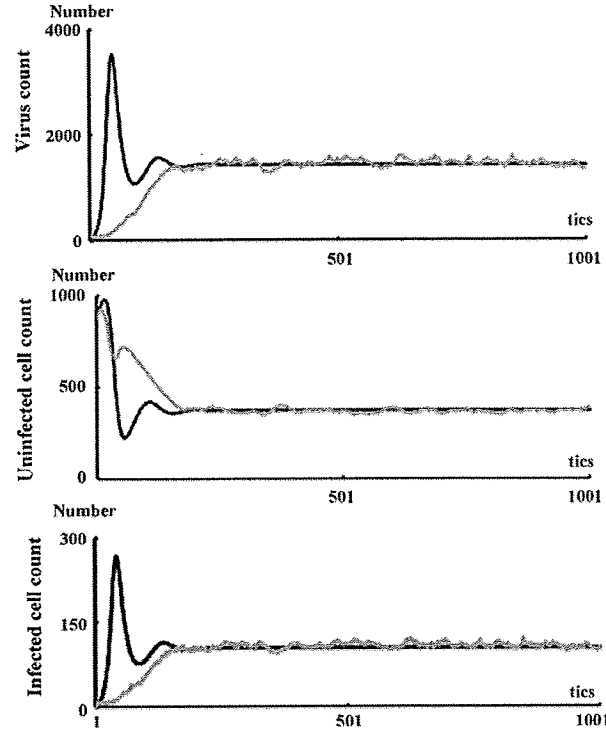

Fig. 3. Comparison of results of agent-based simulation and mathematical simulation. Both sets of results were consistent for the equilibrium phase, but differed in the shift in transition phase. Black line: mathematical model; grey line: results of simulation in RePast. Parameter values were set as follows: initial virus count, 100; uninfected cell count, 880; infected cell count, 0; virus speed of movement, 5 grids/tic; infection rate, 10%; uninfected cell regeneration rate, 1%; latent period, 3 tics; virus reproduction rate, 5/cells/tic; virus lifespan, 10 tics; uninfected cell lifespan, 50 tics; and cell lifespan-shortening ratio as a result of infection, 69%.

$$\frac{dV}{dt} = pI - cV \quad (3)$$

where, T is the uninfected cell count, I is the infected cell count, and V is the virus count. Uninfected cells are supplied to the space with a probability $s[2601 - (T+I)]$, as the number of grids in this agent-based simulation model was 2601 (51 × 51). The death rate of uninfected cells is d, the death rate of infected cells is δ, and the death rate of viruses is c. The infection rate is indicated by β. Viruses are released from infected cells at a probability p.

2.7. Statistical Analysis

Statistical analyses were performed by statistical tests using the program StatView 5.0 (SAS Institute Inc.). All tests of significance were two-tailed, with p values of <0.05 considered to be significant.

3. Results

3.1. Reproducibility of Chronic Viral Infection Disease Models Using Agent-based Simulation Methods

We constructed the chronic viral infection model with StarLogo library. Fig. 1c shows the simulation screen, and Fig. 1e shows one sample result. Immediately after the start of the simulation, the virus count temporarily dropped in accordance with the onset of an infection. Subsequently, the virus count started to increase with an increase in the infected cells and a decrease in the uninfected cells. After a certain number of tics (around 300 in this example), although the virus count, infected cell count, and uninfected cell count had some fluctuation, an equilibrium state was reached. We use the following descriptive terms in this paper: the transient phase is the period during which virus growth peaks, and the equilibrium phase is the period during which an equilibrium state is

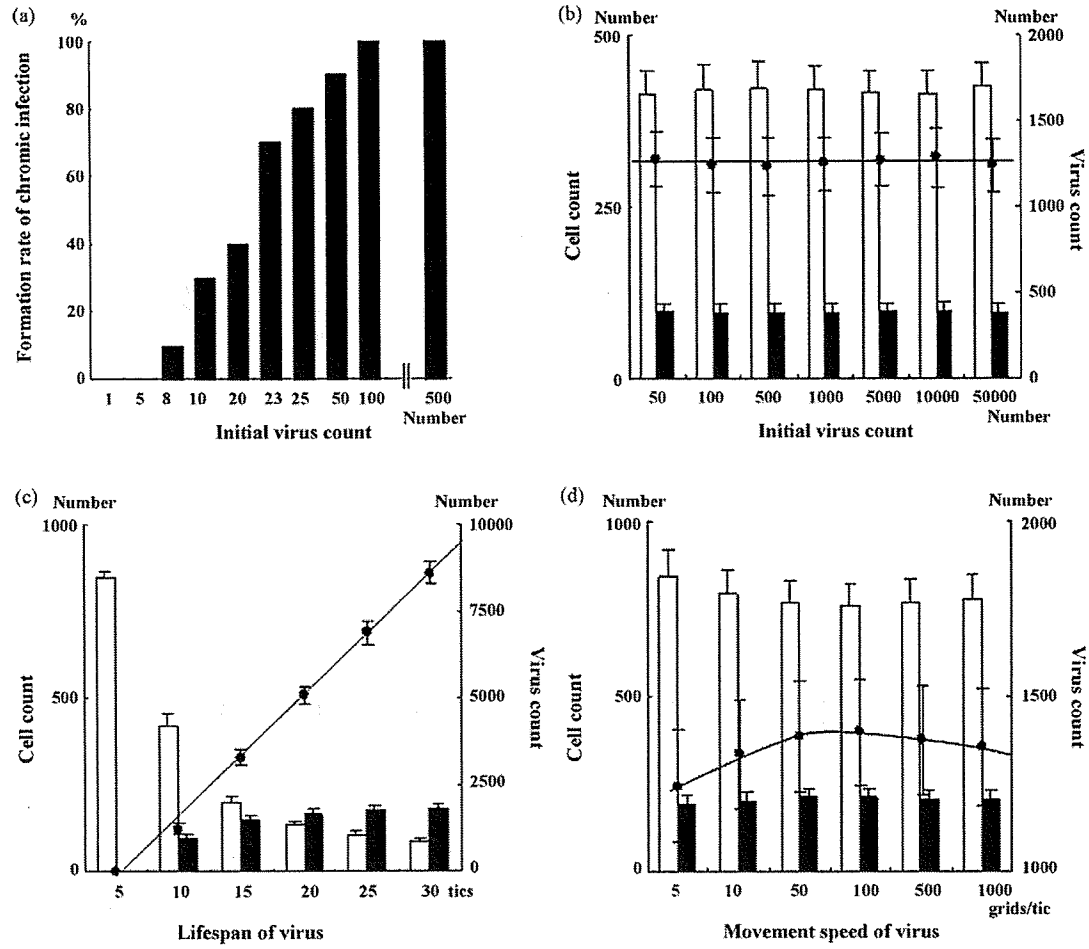

Fig. 4. Effects of changes in viral parameters. (a) The higher the initial virus count, the greater is the increase in the rate of formation of chronic infection, but (b) there was no effect on the conditions in the equilibrium phase. (c) Extending the virus lifespan increased the virus count. (d) Increasing the speed of virus movement to 100 grids/tic increased the virus count, but increasing it to 500 grids/tic had the opposite effect, with a slight declining trend. (a) Black bars: number of infections produced; (b–d) black circles: virus count; line: virus count approximation curve; white bars: uninfected cell count; black bars: infected cell count.

established. When the simulation was performed multiple times, the features described above were maintained, and the average values for virus, infected cell, and uninfected cell counts during the equilibrium state were all consistent.

Fig. 1d shows the simulation screen of the RePast. When we attempted setting all the initial parameters to the same values as those in the StarLogo, the results were not consistent. When we recalculated the parameters from the simulation results, in RePast, the parameters were largely maintained at the levels of the settings, but in StarLogo, the lifespans of both cell types became shorter than the settings while the simulation was in progress. We made the results of both simulations consistent by using the same parameters during the actual simulation (Fig. 2a and b).

3.2. Comparison Between Agent-based Simulation Models and Mathematical Simulation Model

We investigated whether the results of a chronic viral infection disease model produced by RePast would be consistent with the results of a mathematical model. For the mathematical model, we carried out an approximate integration using a four-dimensional Runge–Kutta method to ensure that the uninfected cell count and infected cell count would be in the same class. Parameters were always fixed as constant between simulations. The simulation results were consistent for the equilibrium phase, but transitions in virus count during the transient phase varied, with a shift to equilibrium state following two overshoots in the mathematical model, but a monotonic increase following a logistic curve in the agent-based model (Fig. 3). In the mathematical model, when the equilibrium condition was calculated with $dT/dt = dI/dt = dV/dt = 0$, the equilibrium-phase virus count, uninfected cell count, and infected cell count were very similar to those of the agent-based model (virus count: mathematical model 371.8/space, agent-based model 371.1 ± 32.4/space [average ± SD]; uninfected cell count: mathematical model 1605/space, agent-based model 1454 ± 194/space; infected cell count: mathematical model 115.9/space, agent-based model 108.3 ± 14.2/space).

3.3. Usability of the Models; Effect of Changing Parameters

We investigated the changes in the equilibrium phase brought about by changing each parameter. All the investigations below were carried out by using RePast, and we used the average values from ten simulations.

3.4. Viral Parameters

The lower the virus counts at the beginning of the simulation, the lower the probability of a chronic infection (Fig. 4a). However, the initial virus count did not have any effect on the equilibrium

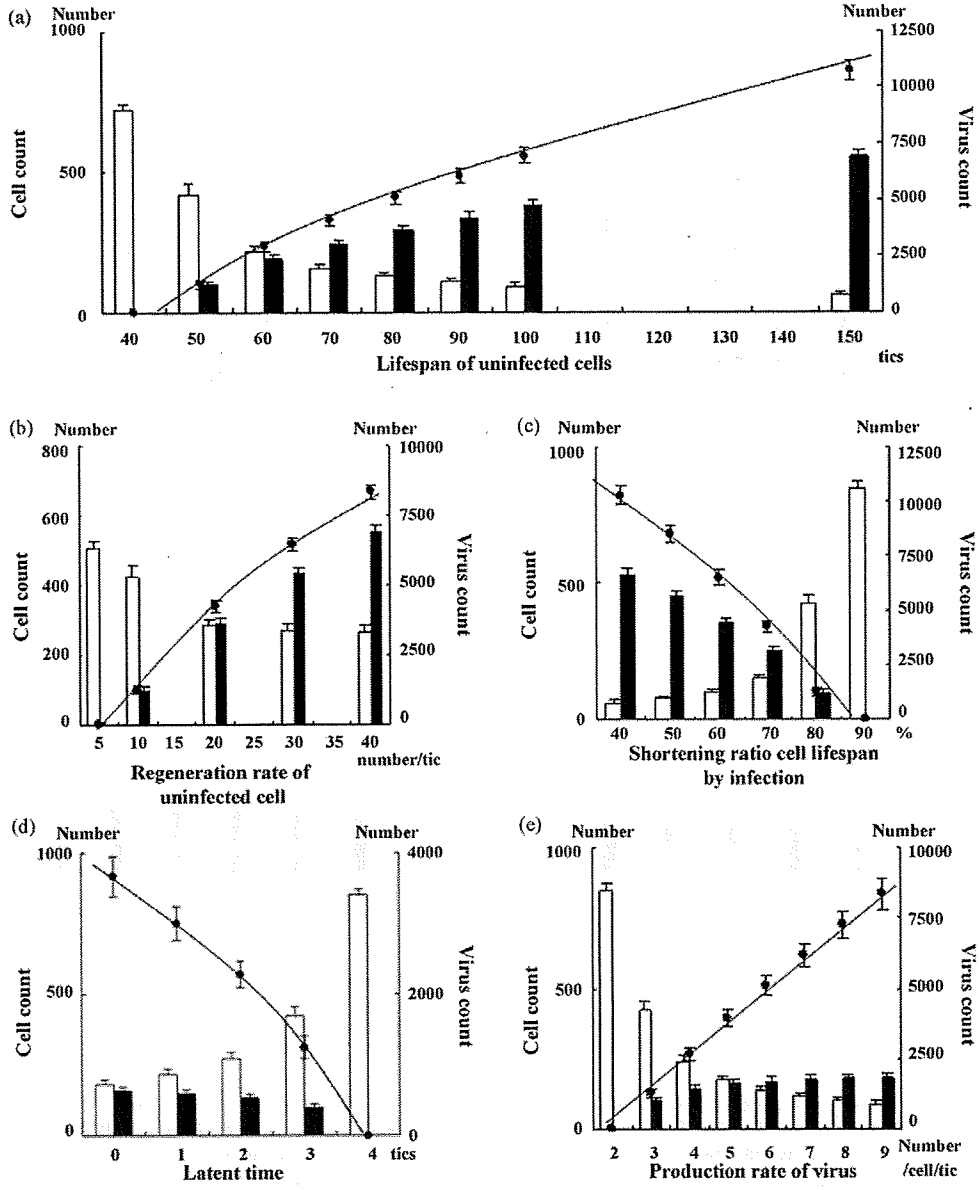

Fig. 5. Effects of changes in cell parameters. (a) Extending the uninfected cell lifespan and (b) increasing the uninfected cell regeneration rate increased the virus count. (c) Raising the lifespan-shortening ratio as a result of infection shortened the lifespan of infected cells, thereby decreasing the virus count. (d) Extending the latent period shortened the period of virus production from infected cells, thereby decreasing the virus count. (e) Increasing the virus production count resulted in a linear increase in equilibrium-phase virus count. Black circles: virus count; line: virus count approximation curve; white bars: uninfected cell count; black bars: infected cell count.

phase itself (Fig. 4b). Extending the lifespan of viruses resulted in a linear increase in equilibrium-phase virus count (Fig. 4c). Although the infected cell count increased, the rate of increase gradually declined. Changing the speed of viral movement resulted in the equilibrium-phase virus count to eventually decline after 100 grids/tic was reached, allowing movement over an area twice the size of the simulation space (Fig. 4d).

3.5. Uninfected Cell Parameters

Extending the lifespan of uninfected cells led to an increased virus count during the equilibrium phase (Fig. 5a). Increasing the uninfected cell regeneration rate also contributed to increased equilibrium-phase virus count (Fig. 5b). In both the cases, the increases in virus count and infected cell count were not linear, but showed a tendency for the rate of increase to decline gradually.

3.6. Infected Cell Parameters

We carried out an investigation of the effects of variation in the lifespan-shortening ratio on the virus count on the assumption that cell lifespan is shortened by infection. When this ratio was increased, the virus count decreased (Fig. 5c). An extended latent period was also related to a decreased virus count (Fig. 5d). However, the virus production from infected cells led to a linear increase in the virus count (Fig. 5e).

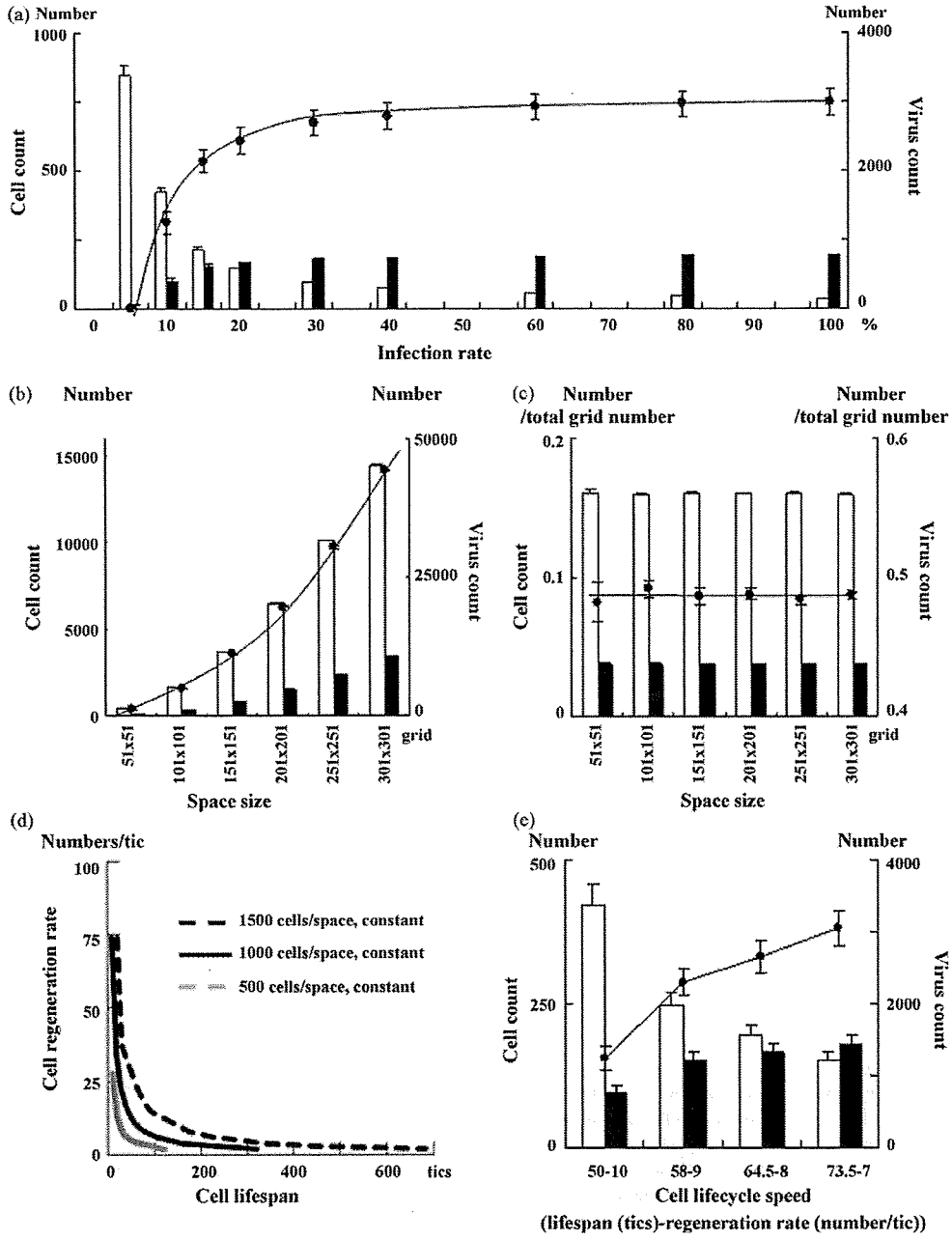

Fig. 6. (a) Increasing the infection rate increased the virus count in equilibrium periods, but the virus count did not change at infection rates of 30% or more. (b) The size of the simulation space increased not only virus count but also the cell count; however, (c) when virus and cell counts were divided by the total number of grids in the space, they were constant for all space sizes. (d) Changing the lifespan and regeneration rate of uninfected cells in opposite directions at the same time makes it possible to change only the cell cycle speed without altering the uninfected cell count. (e) When the cell cycle speed was reduced, the virus count increased toward the right of the graph. This may be because the effect of extending the lifespan of cells exceeds that of reducing their regeneration rate. (a–c and e) Black circles: virus count; line: virus count approximation curve; white bars: uninfected cell count; black bars: infected cell count.

3.7. Infection Rate and Space Size

Increasing the infection rate caused an increase in the virus count, but the change was minimal at an infection rate of 30% or more. The same results were seen for infected cell count, but a decrease in uninfected cell count resulted in a tendency for the infection rate to decrease by up to 60% (Fig. 6a).

The larger the space, higher the increase in both virus and cell counts (Fig. 6b). This increase was proportional to space size, however, when virus and cell counts were divided by the total number of grids in the space they were all constant (Fig. 6c).

3.8. Cell Cycle Speeds

Running a simulation with the initial virus count set to zero enables only the equilibrium condition for uninfected cells to be simulated. Changing the lifespan and regeneration rate of uninfected cells in opposite directions at the same time makes it possible